Supplementary Information

Anisotropic Plasmonic Pd-Tipped Au Nanorods for Near-Infrared Light-Activated Photoacoustic Imaging Guided Photothermal-Photodynamic Cancer Therapy

Chen Yang,[a,b] *Wenli Jiang*,[a] *Yongqi Yu*,[a] *Hui Zhang*,[a,*] *Chenxin Cai*,[a] *Qingming Shen*[b,*]

[a] Jiangsu Key Laboratory of New Power Batteries, Jiangsu Collaborative Innovation Center of Biomedical Functional Materials, Jiangsu Key Laboratory of Biomedical Materials, National and Local Joint Engineering Research Center of Biomedical Functional Materials, College of Chemistry and Materials Science, Nanjing Normal University, Nanjing, 210097, PR China

[b] State Key Laboratory of Organic Electronics and Information Displays & Jiangsu Key Laboratory for Biosensors, Institute of Advanced Materials (IAM), Nanjing University of Posts & Telecommunications, Nanjing 210023, PR China.

Corresponding Authors

*E-mail: zhangh@njnu.edu.cn (H. Zhang)

*E-mail: iamqmshen@njupt.edu.cn (Q.M. Shen).

Calculation of Photothermal Conversion Efficiency

To investigate the photothermal conversion effect, aqueous solutions of Au, PCA NRs and PTA NRs (50 μg mL^{-1}) were irradiated with the 808 nm laser for 600 s (0.75 W cm^{-2}), and then the NIR laser was turned off. An infrared thermal camera was used to measure the real-time temperature of different solutions, and the change in temperature was recorded every 20 s.

The photothermal conversion efficiency (η) of Au NRs, PCA NRs and PTA NRs can be calculated according to the equation[1] (eq 1)

$$\eta = \frac{hS(T_{max} - T_{surr}) - Q_{dis}}{I\left(1 - 10^{-A_{808}}\right)} \quad (1)$$

where T_{max} (K) means the equilibrium temperature; T_{surr} (K) is the ambient temperature of the surroundings. Q_{dis} (W) represents the heat transferred from the light to the container, and it was calculated to be approximately equal to 0 mW. Symbol I (W cm^{-2}) represents the incident laser power density; A_{808} is the absorbance of the sample at 808 nm. The h (W cm^{-2} K^{-1}) refers to the heat transfer coefficient, S (cm^2) represents the surface area of the container, and hS can be calculated by the following equation (eq 2)

$$\tau_s = \frac{m_D c_D}{hS} \quad (2)$$

where τ_s is the sample system time constant; m_D and c_D are the mass (0.6 g) and heat capacity (4.2 J g^{-1} $^oC^{-1}$) of the solvent.

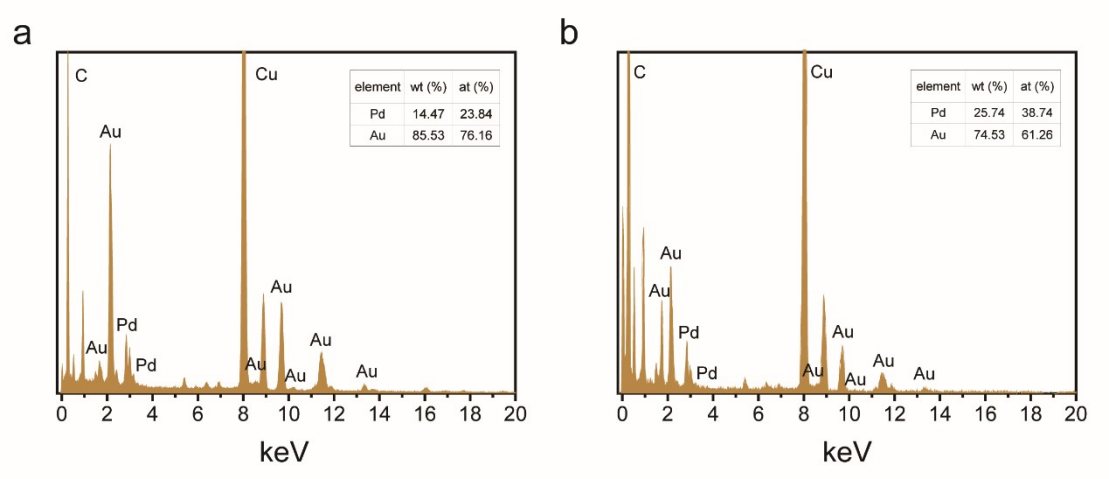

Fig. S1. EDS of PTA NRs (a), PCA NRs (b).

Table S1. The elemental wt% for PTA and PCA NRs measured by ICP-AES.

element	PTA (%)	PCA (%)
Pd	19.09	22.95
Au	80.91	77.05

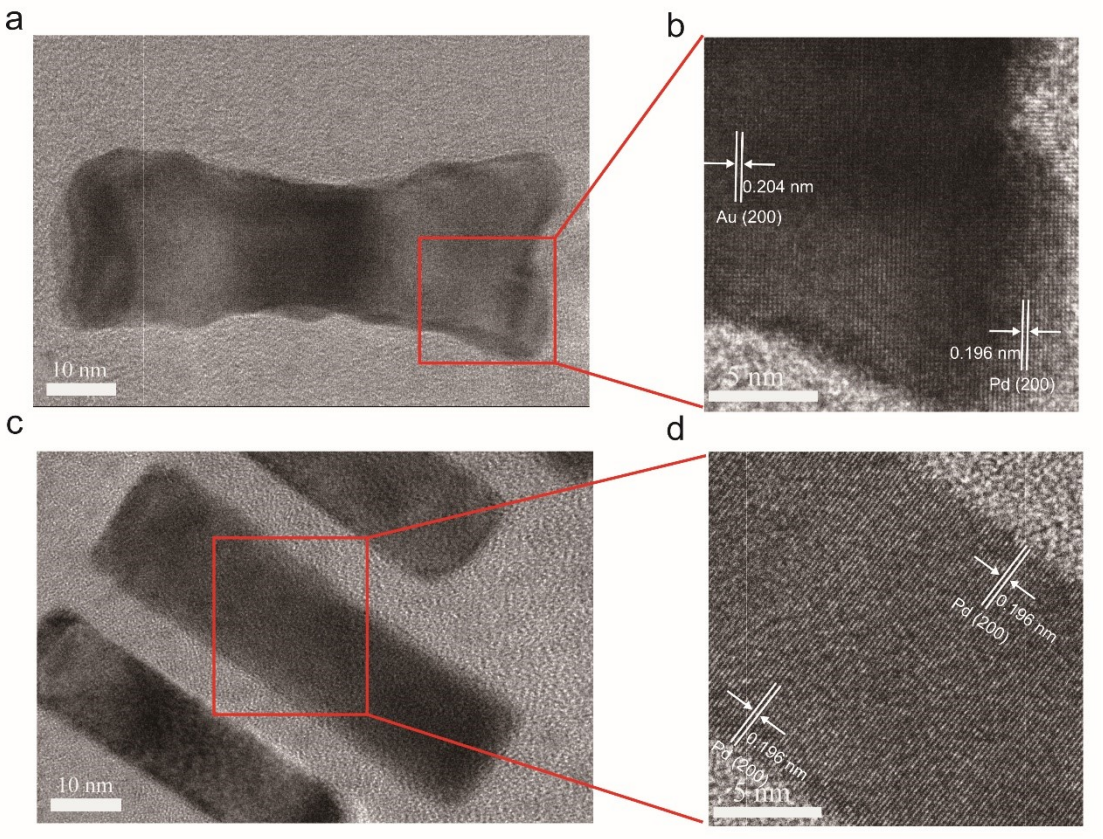

Fig. S2. (a) TEM and (b) HRTEM images of PTA NRs. (c) TEM and (d) HRTEM images of PCA NRs.

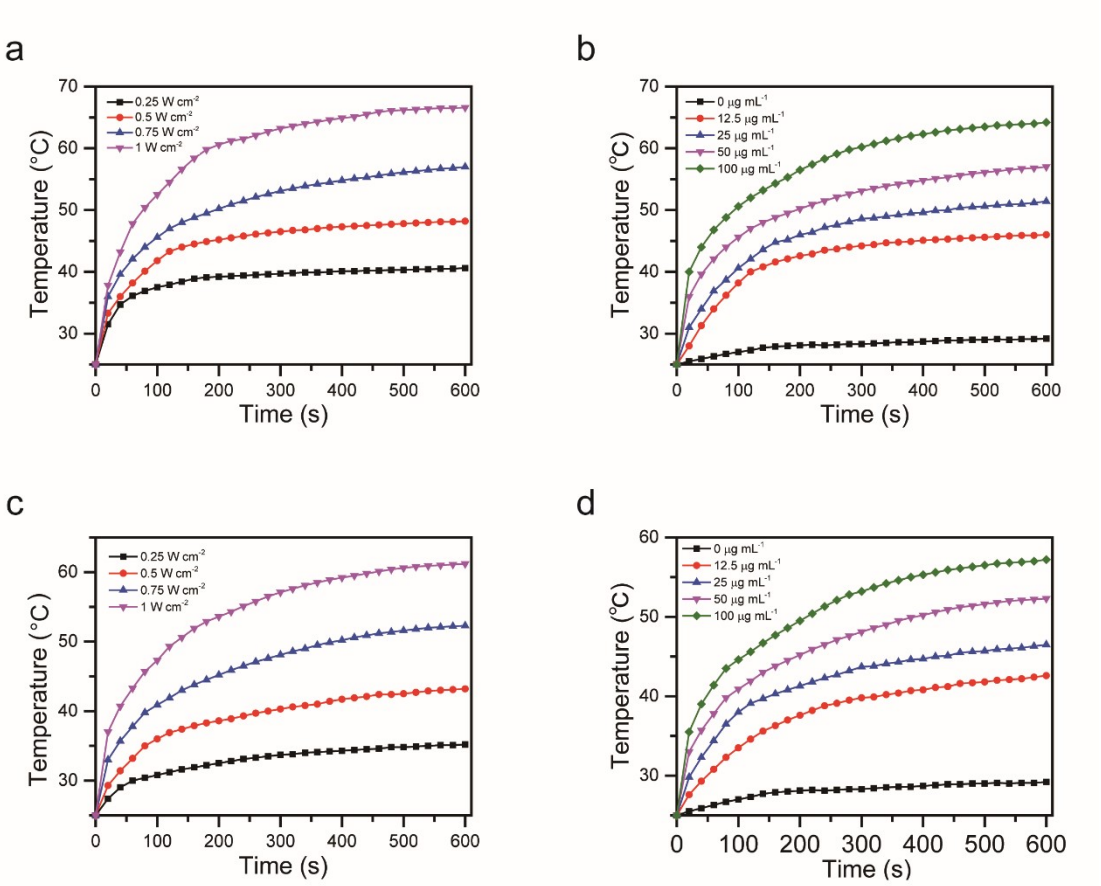

Fig. S3. Temperature increases of PTA NRs (a) and PCA NRs (c) solution under 808 nm laser irradiation at different laser power for 600 s (50 μg mL^{-1}). Temperature increases of PTA NRs (b) and PCA NRs (d) solution with different concentrations under 808 nm laser (0.75W cm^{-2}) irradiation for 600 s.

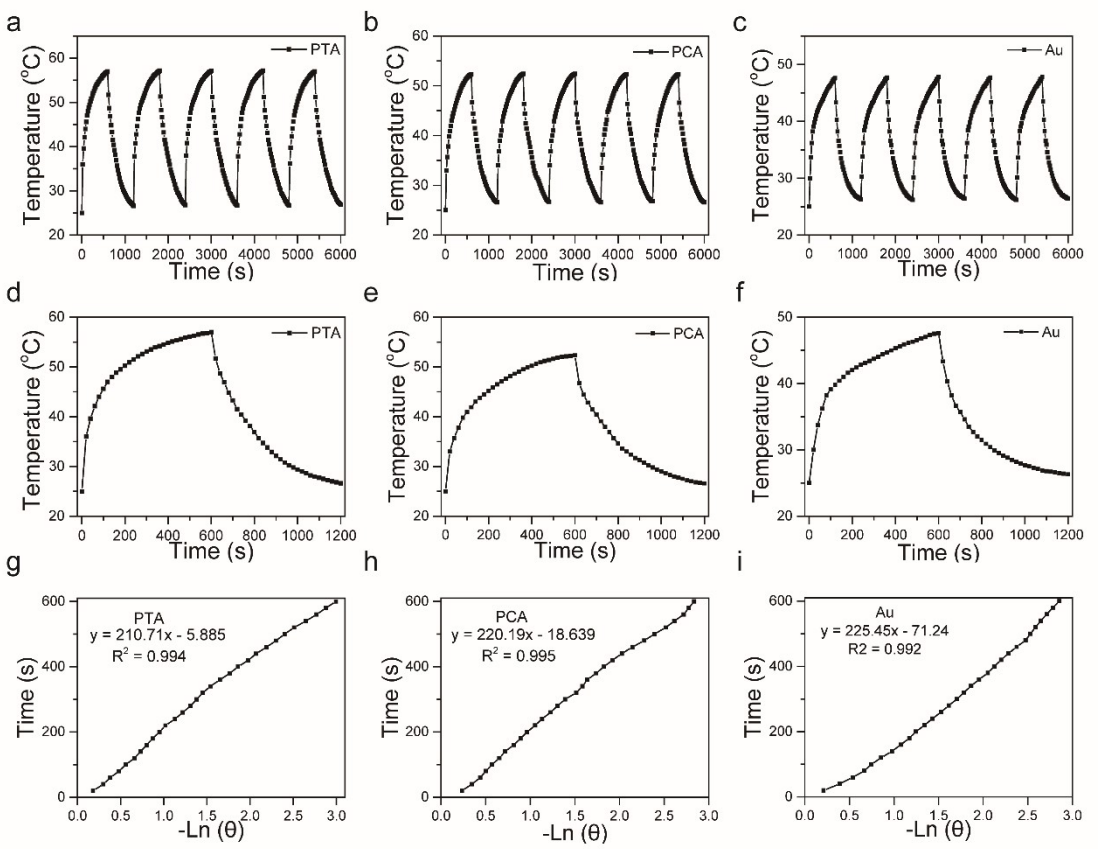

Fig. S4. Cycle curve of temperature for PTA NRs (a), PCA NRs (b), Au NRs (c) (equivalent to 50 μg mL^{-1} Au) under 808 nm laser irradiation (0.75W cm^{-2}). The temperature variation curves of PTA NRs (d), PCA NRs (e), Au NRs (f) under 808 nm laser irradiation (0.75W cm^{-2}) for 600 s, followed by natural cooling with laser switched off for 600 s. The linear regression curves of PTA NRs (g), PCA NRs (h), Au NRs (i).

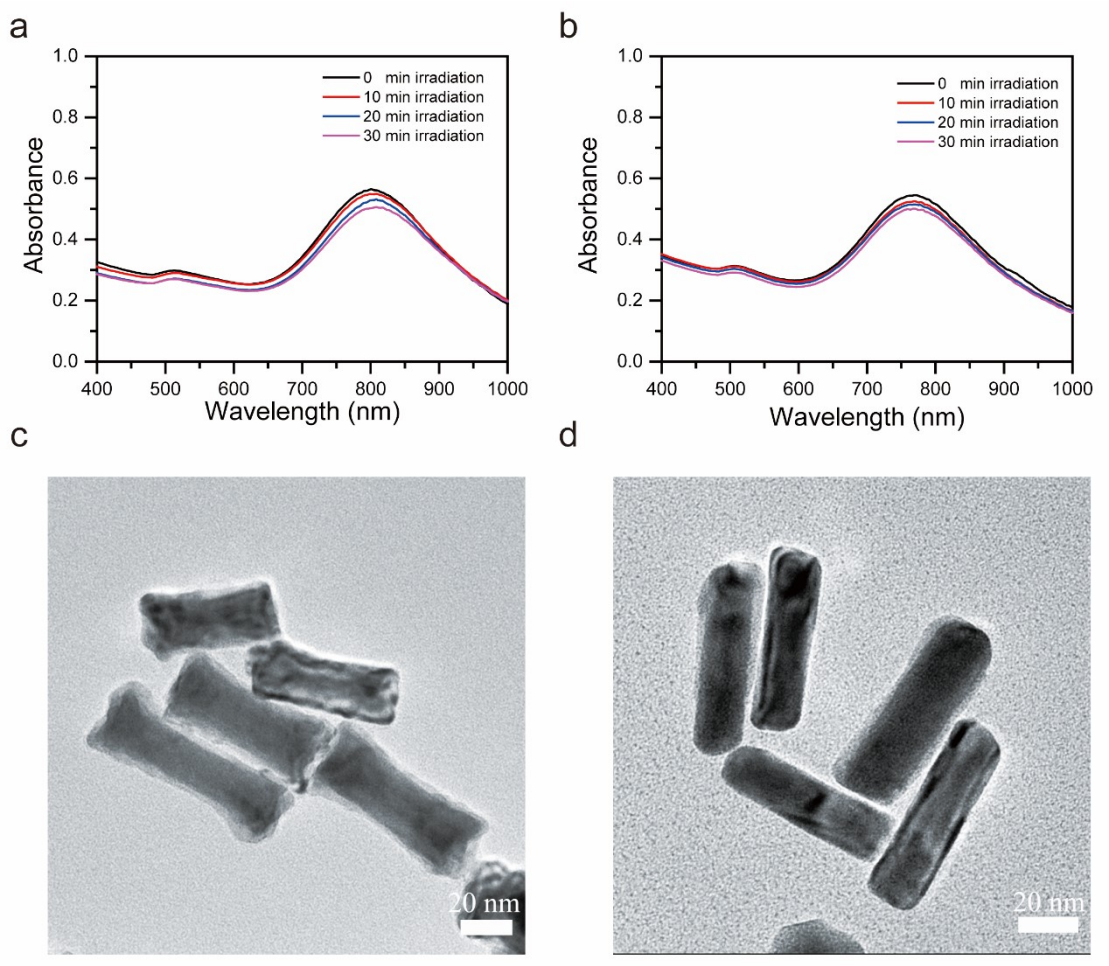

Fig. S5. The photostability of PTA NRs and PCA NRs. UV-vis-NIR absorption spectra of PTA NRs (a) and PCA NRs (b) exposed to 808 nm laser at 0.75 W cm^{-2} for different time points. TEM images of PTA NRs (c), PCA NRs (d) exposed to 808 nm laser at 0.75 W cm^{-2} for 30 min.

Table S2. The heat conversion efficiency of Au, PCA and PTA NRs.

	$T_{max} - T_{surr}$	A_{808}	τ_s	η (%)
Au	22.6	0.52	225.45	48.1
PCA	26.3	0.72	220.19	51.4
PTA	32	1.16	210.71	54.8

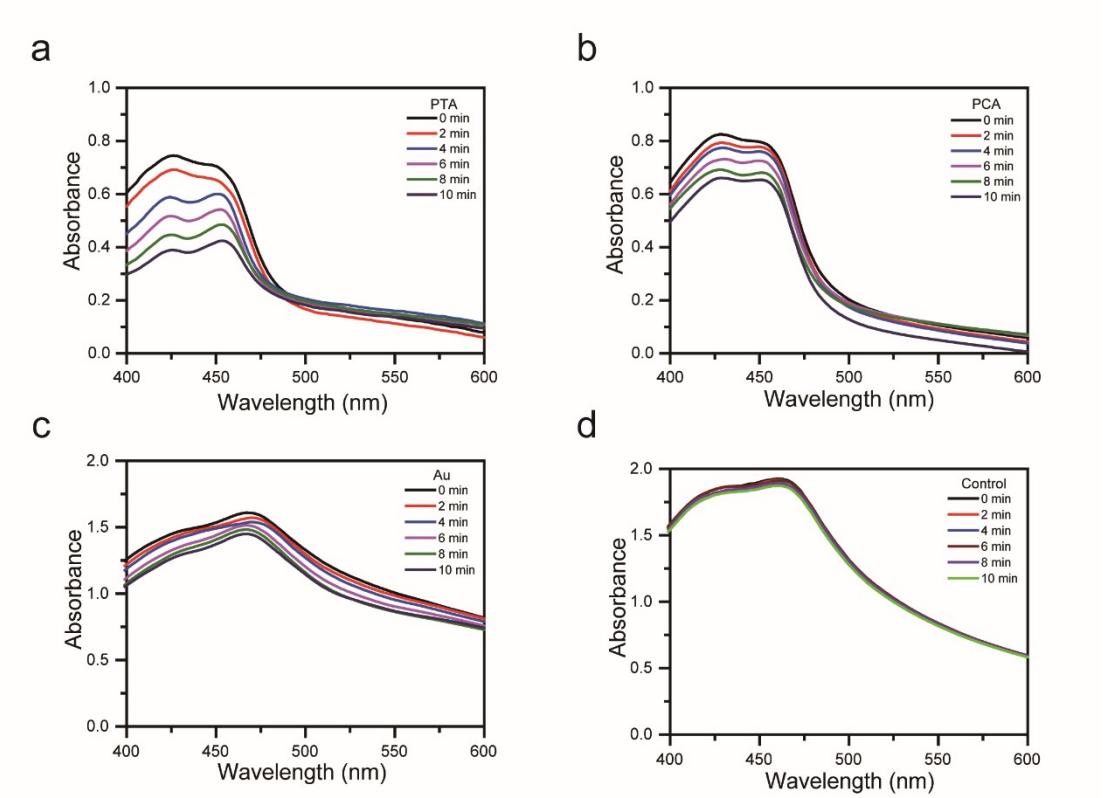

Fig. S6. Time-dependent UV-vis absorption spectra of DPBF in different solutions under 808 nm laser irradiation (0.75 W cm^{-2}). PTA NRs (a), PCA NRs (b), Au NRs (c), H_2O (d).

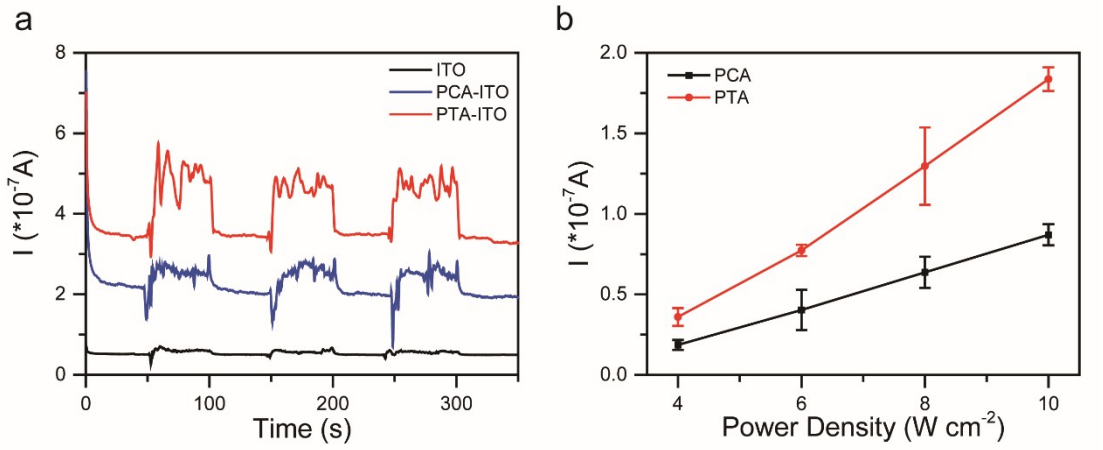

Fig. S7. (a) The switching cycles of the photocurrent signal of the PTA NR-modified ITO or PCA NR-modified ITO or bare ITO electrode under laser (808 nm) irradiation, respectively. (b) Photocurrent signal of PTA NR-modified ITO or PCA NR-modified ITO under laser (808 nm) irradiation at different power densities.

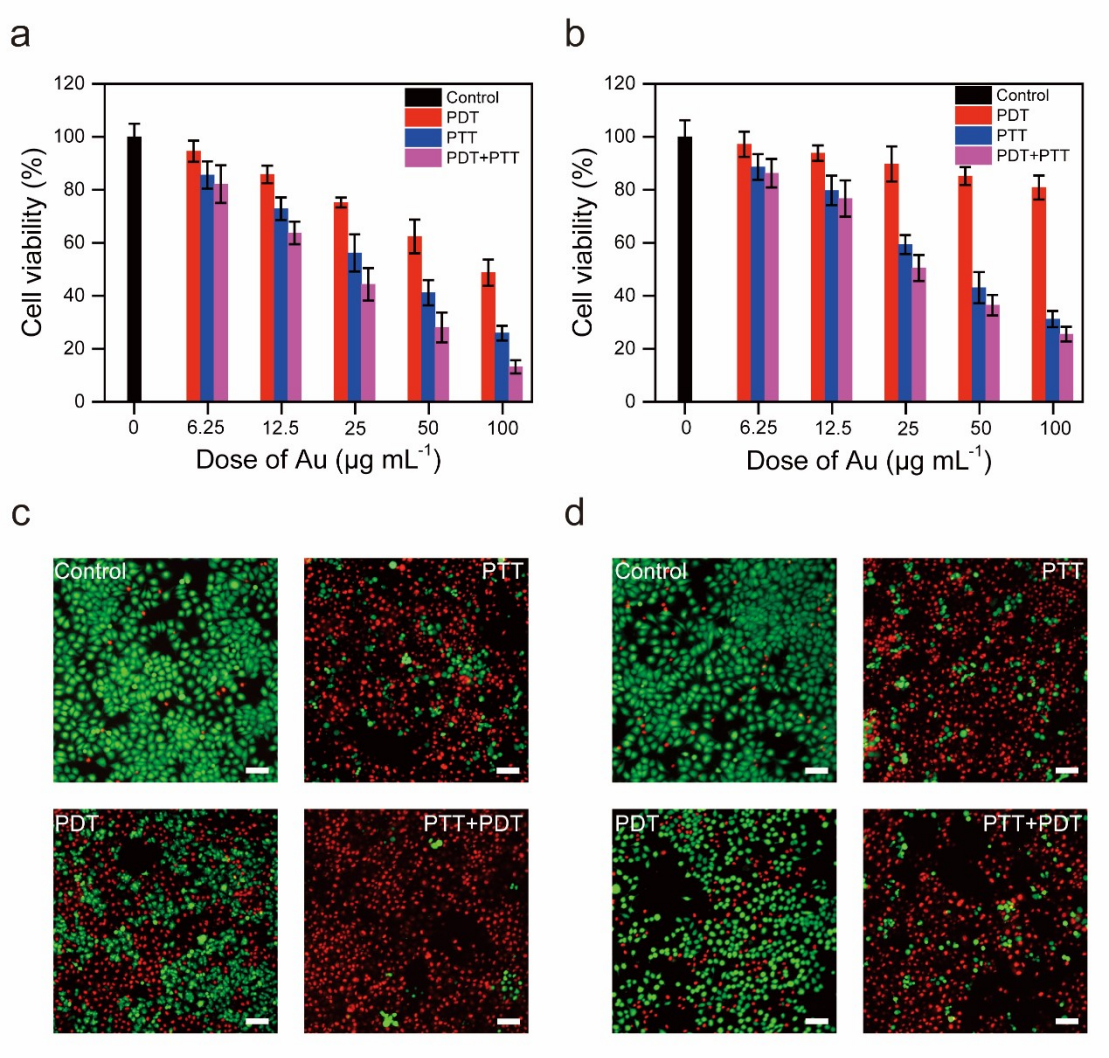

Fig. S8. Cell viability of MCF-7 cells treated with PTT, PDT and PTT + PDT incubated with PTA NRs (a) or PCA NRs (b) under laser irradiation. Fluorescent images of live/dead staining of MCF-7 cells treated by PTT, PDT and PTT + PDT incubated with PTA NRs (c), PCA NRs (d). The dead cells were stained red, living cells were stained green. Scale bars, 200 μm.

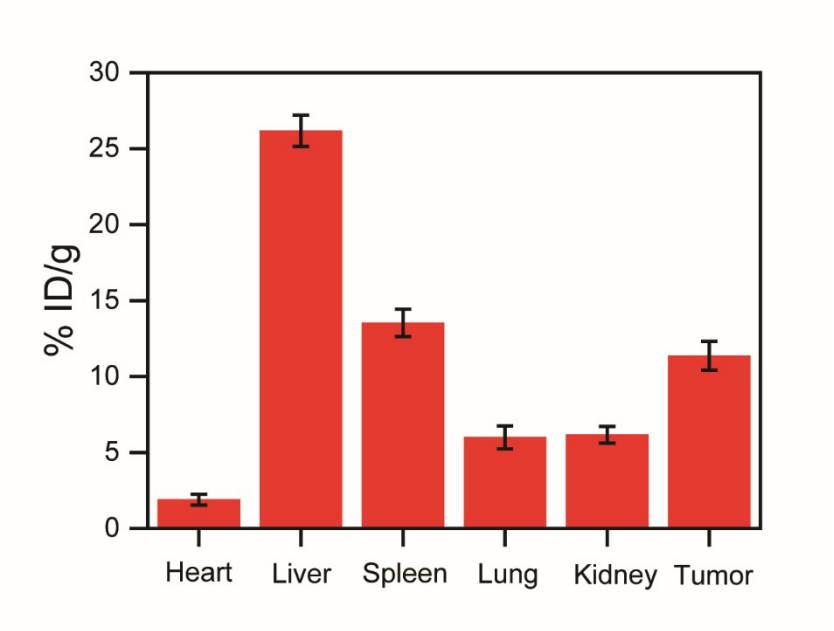

Fig. S9. Biodistribution of PTA NRs in main tissues and tumor 24 h after intravenous injection.

Table S3. The main parameters of blood biochemistry and routine testing for mice treated with PTA NRs.

Parameter	Unit	Control	PTA NRs	Reference
WBC	10^9/L	6.4	6.8	0.8-6.8
Lymph	10^9/L	1.7	2.3	0.7-5.7
Mon	10^9/L	0.1	0.2	0.0-0.3
Gran	10^9/L	0.3	0.1	0.1-1.8
Lymph	%	61.8	64.8	55.8-90.6
Mon	%	4.3	4.4	1.8-6.0
Gran	%	18.6	22.6	8.6-38.9
RBC	10^{12}/L	7.54	7.14	6.36-9.42
HGB	g/L	135	141	110-143
HCT	%	42.1	42.9	34.6-44.6
MCV	fL	55.9	53.5	48.2-58.3
MCH	pg	15.9	16.6	15.8-19
MCHC	g/L	337	384	302-353
RDW	%	14.2	15.9	13-17
PLT	10^9/L	617	626	450-1590
MPV	fL	6.1	4.7	3.8-6.0
PDW		15.1	16.6	
PCT	%	0.581	0.672	

REFERENCES

(1) M. Chang, Z. Hou, M. Wang, M. Wang, P. Dang, J. Liu, M. Shu, B. Ding, A.A. Al Kheraif, C. Li, J. Lin, Cu_2MoS_4/Au heterostructures with enhanced catalase-like activity and photoconversion efficiency for primary/metastatic tumors eradication by phototherapy-induced immunotherapy, Small. 16 (2020) 1907146.